JACS
JOURNAL OF THE AMERICAN CHEMICAL SOCIETY

Article

pubs.acs.org/JACS

Electrocatalytic Alcohol Oxidation with Ruthenium Transfer Hydrogenation Catalysts

Kate M. Waldie, Kristen R. Flajslik, Elizabeth McLoughlin, Christopher E. D. Chidsey, and Robert M. Waymouth*

Department of Chemistry, Stanford University, Stanford, California 94305, United States

Supporting Information

ABSTRACT: Octahedral ruthenium complexes [RuX(CNN)(dppb)] (**1**, X = Cl; **2**, X = H; CNN = 2-aminomethyl-6-tolylpyridine, dppb = 1,4-bis(diphenylphosphino)butane) are highly active for the transfer hydrogenation of ketones with isopropanol under ambient conditions. Turnover frequencies of 0.88 and 0.89 s^{-1} are achieved at 25 °C using 0.1 mol % of **1** or **2**, respectively, in the presence of 20 equiv of potassium *t*-butoxide relative to catalyst. Electrochemical studies reveal that the Ru−hydride **2** is oxidized at low potential (−0.80 V versus ferrocene/ferrocenium, $Fc^{0/+}$) via a chemically irreversible process with concomitant formation of dihydrogen. Complexes **1** and **2** are active for the electrooxidation of isopropanol in the presence of strong base (potassium *t*-butoxide) with an onset potential near −1 V versus $Fc^{0/+}$. By cyclic voltammetry, fast turnover frequencies of 3.2 and 4.8 s^{-1} for isopropanol oxidation are achieved with **1** and **2**, respectively. Controlled potential electrolysis studies confirm that the product of isopropanol electrooxidation is acetone, generated with a Faradaic efficiency of 94 ± 5%.

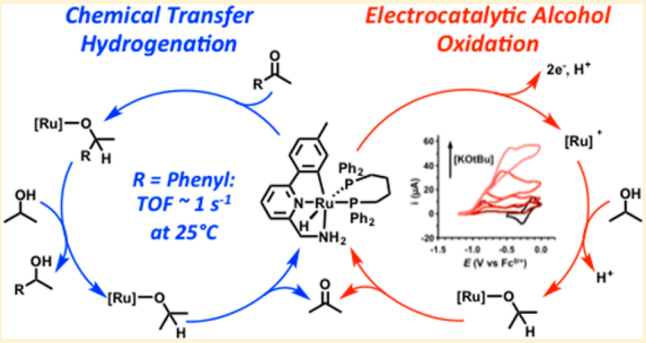

INTRODUCTION

The transition to a renewable energy economy will require the storage of energy from renewable energy resources such as solar and wind power in chemical fuels, and the efficient extraction of useable energy from these fuels on demand. Carbon-based fuels are well suited to function as large-scale energy carriers because of their high energy densities. In particular, liquid fuels such as alcohols offer obvious safety and handling advantages and can be stored and delivered using established infrastructure.[1−4]

The production of liquid fuels using renewable energy via reduction of carbon dioxide has been proposed as a means to address the first half of this energy cycle, that is, fuel generation.[5−9] To this end, chemical[10−24] and electrocatalytic[25,26] hydrogenation of CO_2 to liquid products with homogeneous transition metal complexes has been the focus of much recent research. For the second half of the cycle, combustion remains the primary method for harvesting energy from carbon fuels on a global scale, particularly in the transportation sector.[27] However, combustion engines are thermodynamically wasteful, with most of the generated energy being lost as heat. Fuel cells are a promising alterative to combustion engines due to their significantly higher theoretical efficiencies. Vehicles powered by hydrogen fuel cells are now being offered in select regions,[28] although hydrogen gas presents many difficulties as a chemical fuel.[4] Direct alcohol fuel cells are also being explored, but their efficiency is severely limited by the high overpotentials required to generate reasonable currents even with the most optimized heterogeneous electrooxidation catalysts.[3,29]

The electrochemical oxidation of alcohols using molecular Ru poly pyridyl catalysts has been extensively explored,[30−32] but high overpotentials are required to generate the key Ru−oxo active catalyst. Transfer hydrogenation[33,34] of carbonyl substrates with alcohol hydrogen donors using metal−hydride catalysts represents a promising strategy for the discovery of systems capable of energy-efficient electrocatalytic alcohol oxidation.[35−38] The rapid formation of a metal−hydride from the alcohol donor during transfer hydrogenation implies that the metal−hydride bond is readily generated near the reversible thermodynamic potential for alcohol oxidation. The conversion of a chemical transfer hydrogenation cycle into an electrocatalytic scheme for alcohol oxidation requires replacement of the ketone substrate with an electrode as the terminal oxidant (Figure 1).

We previously reported on a class of Ru^{II} transfer hydrogenation catalysts[33,34] that are active for electrocatalytic alcohol oxidation in aqueous solution (pH 11.5) when physisorbed onto edge-plane graphite electrodes.[36] Electrocatalytic conversion of methanol to formate was observed at a rate of 1.35 M^{-1} s^{-1}, but at very positive potentials (ca. 0.6 V versus NHE, pH 11.5). Mechanistic studies implicated a Ru−

Received: September 20, 2016
Published: December 20, 2016

DOI: 10.1021/jacs.6b09705
J. Am. Chem. Soc. 2017, 139, 738−748

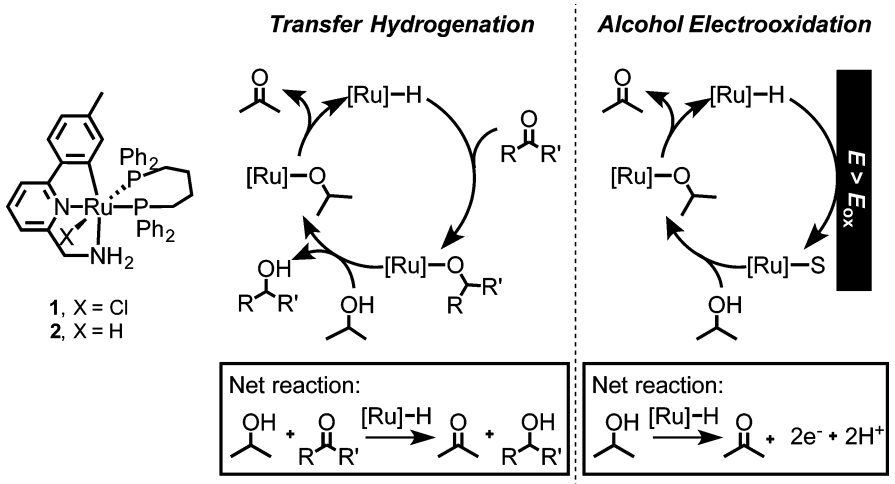

Figure 1. Left: Ruthenium complexes **1** and **2**. Center: Transfer hydrogenation of ketones with Ru−hydride catalyst **2**. Right: Proposed electrocatalytic alcohol oxidation using the Ru−hydride catalyst **2**.

oxo species[32] as the active catalyst instead of the targeted Ru−hydride cycle.

Herein, we examine the electrocatalytic oxidation of isopropanol with Ru−chloride **1** and Ru−hydride **2**, one of the most efficient systems reported for ketone transfer hydrogenation in refluxing isopropanol (Figure 1).[39,40] We demonstrate that these complexes maintain their high activity for transfer hydrogenation under ambient conditions. Detailed kinetic studies suggest a complicated rate law in which reversible substrate inhibition occurs with enolizable ketones. The Ru−hydride **2** exhibits a low-potential, chemically irreversible oxidation by cyclic voltammetry, which changes from a one-electron to a two-electron process upon the addition of potassium *t*-butoxide. In the presence of isopropanol under strongly basic conditions, complexes **1** and **2** exhibit rapid turnover frequencies for the two-electron electrocatalytic oxidation of isopropanol to acetone with a maximum current enhancement at approximately −0.5 V versus ferrocene/ferrocenium ($Fc^{0/+}$) in tetrahydrofuran.

RESULTS AND DISCUSSION

Synthesis and Characterization. The Ru−chloride **1**[39,41] and Ru−hydride **2**[35,38] were synthesized as previously described. The Ru−phenoxide **3** was prepared as an isolable analogue of the Ru−isopropoxide species. Treatment of **1** with phenol in the presence of potassium *t*-butoxide in tetrahydrofuran yields the Ru−phenoxide **3**, which is isolated as an orange powder. The ^{31}P NMR of **3** displays two sets of doublet at δ_P 61.2 and 39.4 ppm with $^2J(PP)$ = 35.1 Hz, comparable to the coupling constants observed for other Ru−OR complexes in this family.[41,42]

Crystals of **3** suitable for X-ray diffraction were obtained by slow evaporation of a saturated *p*-xylene solution. The ruthenium center in **3** is in a distorted octahedral geometry with the tridentate CNN ligand and bidentate phosphine ligand (Figure 2), similar to the solid-state structures of **1**[39] and other closely related complexes.[42,43] The Ru−O bond length of 2.165 Å for **3** is comparable to those of the Ru−formate and Ru−acetate complexes.[42]

Catalytic Transfer Hydrogenation. The transfer hydrogenation of acetophenone with **1** and **2** in isopropanol was investigated under identical conditions (Scheme 1). Turnover

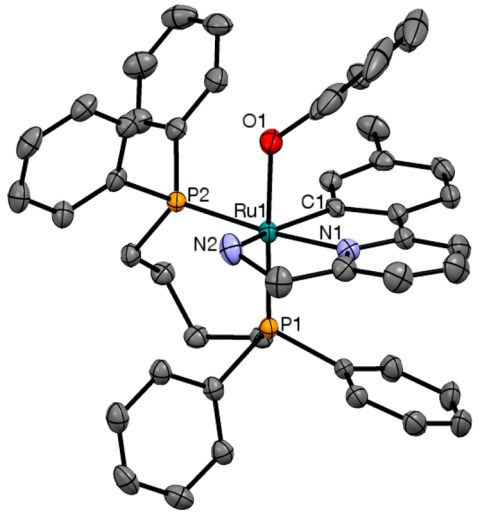

Figure 2. Structure of **3**, 50% probability ellipsoids. Hydrogen atoms are omitted for clarity. Selected bond distances (Å) and angles (deg): Ru1−C1 2.052(4), Ru1−N1 2.060(3), Ru1−N2 2.224(4), Ru1−P1 2.233(1), Ru1−P2 2.295(1), Ru1−O1 2.165(3); N1−Ru1−C1 80.2(1), N1−Ru1−N2 76.9(1), N1−Ru1−P1 92.61(9), N1−Ru1−P2 172.6(1), N2−Ru1−C1 155.1(2), N2−Ru1−P1 103.3(1), N2−Ru1−P2 99.1(1), C1−Ru1−P1 87.0(1), C1−Ru1−P2 102.6(1), P1−Ru1−P2 94.40(4), P1−Ru1−O1 176.14(9).

Scheme 1. Transfer Hydrogenation of Acetophenone with Isopropanol Using 1 or 2

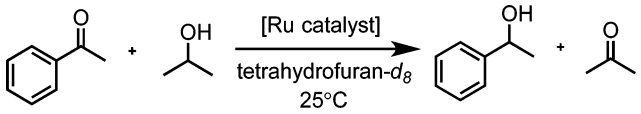

frequencies (TOF) calculated from the initial rates are presented in Table 1, entries 1 and 2. Reactions were performed at 25 °C to mimic our electrochemical conditions (vide infra). Using 0.1 mol % of **1** or **2**, ca. 80% conversion of acetophenone is observed by ^1H NMR within 15 min in tetrahydrofuran-d_8 with 25 equiv of potassium *t*-butoxide relative to catalyst.

The presence of strong base and alcohol is required to activate the Ru−chloride precatalyst **1**,[41] while the Ru−hydride

DOI: 10.1021/jacs.6b09705
J. Am. Chem. Soc. 2017, 139, 738−748

Table 1. Initial Turnover Frequencies for Acetophenone Transfer Hydrogenation[a]

entry	catalyst	[KO^{t}Bu] (M)	TOF (s^{-1})[b]
1	**1**	0.01	0.88
2	**2**	0.01	0.89
3	**2**		0.89

[a]Conditions: 0.1 mol % [Ru], 0.5 M acetophenone, 3.0 M isopropanol in tetrahydrofuran-d_8 with 0.5 M *p*-xylene as an internal standard. [b]TOF = (mmol acetophenone consumed)/(mmol catalyst × time), measured at 900 s.

2 is active in the absence of base. Comparable rates for transfer hydrogenation are observed for **1** plus base and **2** without base (Table 1, entries 1 and 3). Furthermore, the addition of potassium *t*-butoxide to the Ru−hydride **2** does not lead to a rate enhancement for ketone transfer hydrogenation at room temperature, contrary to the observations from Baratta and co-workers[44] that the catalytic rate is increased with **2** in the presence of added base at elevated temperatures.

Kinetic Studies. Investigations into the behavior of **1** and **2** under stoichiometric and catalytic conditions at elevated temperatures have been reported by Baratta.[41,43−45] Detailed studies into the full kinetic profile for transfer hydrogenation at room temperature were undertaken to gain a better understanding of the key chemical steps in the catalytic mechanism under conditions relevant to electrochemical studies.

Organic acids such as acetic acid rapidly protonate the Ru−hydride **2** to generate H_2 and the corresponding Ru−alkoxide.[41] The analogous reaction with unactivated aliphatic alcohols such as isopropanol would provide a scheme for alcohol oxidation in the absence of ketones via acceptorless dehydrogenation.[46] We find that **2** reacts slowly with isopropanol at ambient temperature, yielding a single ruthenium species after 4 h. This product is assigned as the [Ru−isopropoxide][isopropanol] adduct on the basis of the reported ^{31}P NMR data for this species.[45] The formation of H_2 is also confirmed by ^{1}H NMR, which appears as a singlet at δ_H 4.53 ppm.

In light of these results, acceptorless dehydrogenation was examined as a potential competitive pathway under transfer hydrogenation conditions. Beller and co-workers[47] reported acceptorless isopropanol dehydrogenation with **1** in the presence of 2000 equiv of sodium isopropoxide at reflux. Similar results were also obtained with tetrahydro-1-napthol in the presence of potassium *t*-butoxide (50 equiv) in *t*-butanol at 130 °C.[48] However, our transfer hydrogenation conditions were carried out at lower temperatures. The transfer hydrogenation of acetophenone with isopropanol using the Ru−chloride **1** (1 mM) and potassium *t*-butoxide (25 mM) was monitored by ^{1}H NMR at 25 °C, and the concentration of each species was determined (Figure S3). At each time point, the reactant consumption is exactly matched by product formation within experimental error, indicating that acetone production via acceptorless dehydrogenation is negligible under these conditions. Furthermore, no acetone is generated over 24 h in the absence of acetophenone under otherwise identical conditions.

With acceptorless alcohol dehydrogenation eliminated as a relevant competitive reaction, the kinetic profile of transfer hydrogenation was investigated. The transfer hydrogenation of 2-heptanone with isopropanol-d_8 using **2** was selected as a model system for these studies (Scheme 2). The choice of using the Ru−hydride **2** instead of the Ru−chloride **1** removes the need for the addition of alkoxide base, and prevents precatalyst activation from complicating the kinetic analysis. A series of ^{1}H NMR experiments were performed in tetrahydrofuran-d_8 at 25 °C in which the standard conditions (1.3 mM **2**, 0.32 M 2-heptanone, 3.2 M isopropanol-d_8) were varied by changing the concentration of each species individually. Plots of 2-heptanone conversion over time for each run are presented in the Supporting Information: a representative plot for Table 2, entry 2 is shown in Figure 3a. In each case, conversion of 2-heptanone follows a single exponential decay, and the observed rate constants k_{obs} are summarized in Table 2.

Under these conditions, there is a clear first-order dependence of k_{obs} on the catalyst concentration (Figure 3b). This result is in agreement with previous studies, where the transfer hydrogenation of acetophenone was found to be first-order in [**1**] at high base concentration.[44] The observed reaction rate is zero-order in isopropanol-d_8 (Figure S22), which is present in 10-fold excess relative to substrate. Negative order dependences on both of the products, acetone and 2-heptanol (Figures S23 and S24), are consistent with this being an equilibrium reaction, and may suggest a more complicated rate law in which product terms are present in the denominator.[49] Unexpectedly, the plot of k_{obs} versus [2-heptanone] is not linear and does not pass through the origin (Figure 3c). A faster reaction rate is achieved with lower substrate concentrations, indicative of reversible substrate inhibition.

Substrate inhibition has been reported with other bifunctional catalysts for H_2[50,51] and transfer[52] hydrogenation. For these systems, it was posited that a metal−amide intermediate reversibly forms an adduct with the ketone substrate, from which deprotonation of the ketone by the basic amide ligand site may occur to generate an enolate complex. This reversible reaction is fast relative to product formation, resulting in an off-path equilibrium that depends on the substrate concentration.

Evidence of enolate formation with the Ru−hydride **2** is revealed by incorporation of deuterium into the ketone substrate under catalytic conditions. In isopropanol-d_8, 53% and 47% deuterium is observed at the β-methyl and methylene positions of 2-heptanone, respectively, after 6 min, while only 35% conversion to the product 2-heptanol has occurred by this point (Scheme 3). This rapid deuteration of the substrate suggests that fast and reversible formation of the 2-heptanone enolate occurs during transfer hydrogenation. Similar results are obtained when the Ru−phenoxide **3** is treated with 2-heptanone in the presence of isopropanol-d_8. In both cases, deuteration of the substrate suggests that the catalyst is operating under basic conditions, despite the absence of added base. This behavior may be attributed to ionization of the Ru−

Scheme 2. Transfer Hydrogenation of 2-Heptanone with Isopropanol-d_8 Using 2

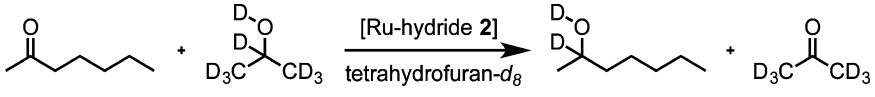

DOI: 10.1021/jacs.6b09705
J. Am. Chem. Soc. 2017, 139, 738−748

Table 2. Kinetic Data for the Transfer Hydrogenation of 2-Heptanone with Isopropanol-d_8 Using 2[a]

entry	[2] (mM)	[2-heptanone] (M)	[isopropanol-d_8] (M)	[2-heptanol] (M)	[acetone] (M)	k_{obs} (10^{-3} s^{-1})[b]
1	0.63	0.32	3.16			0.68 ± 0.07
2	1.26	0.32	3.16			1.26 ± 0.13
3	2.53	0.32	3.16			2.26 ± 0.14
4	3.67	0.32	3.16			3.46 ± 0.20
5	1.26	0.16	9.28			3.29 ± 0.33
6	1.26	0.24	9.28			1.63 ± 0.16
7	1.26	0.32	9.28			1.15 ± 0.11
8	1.26	0.63	9.28			0.63 ± 0.10
9	1.26	0.78	9.28			0.70 ± 011
10	1.26	0.95	9.28			0.56 ± 0.08
11	1.26	0.32	4.68			1.20 ± 0.07
12	1.26	0.32	6.22			1.28 ± 0.08
13	1.26	0.32	3.16	0.10		1.08 ± 0.09
14	1.26	0.32	3.16	0.20		0.89 ± 0.07
15	1.26	0.32	3.16	0.32		0.81 ± 0.06
16	1.26	0.32	3.16		0.11	0.98 ± 0.08
17	1.26	0.32	3.16		0.21	0.80 ± 0.06
18	1.26	0.32	3.16		0.31	0.60 ± 0.05

[a]Conditions: Reactions performed in tetrahydrofuran-d_8 at 25 °C with 0.32 M *p*-xylene as an internal standard. [b]Observed rate constant k_{obs} is obtained from the first-order exponential decay fit of [2-heptanone] versus time plots.

isopropoxide or Ru−phenoxide bond, providing a strong alkoxide base capable of substrate deprotonation in situ. Deuteration of secondary alcohols has been reported by Baratta and co-workers[53] for a series of related ruthenium and osmium complexes, although these experiments were performed in the presence of excess alkoxide base.

The transfer hydrogenation of benzophenone, a non-enolizable substrate, in isopropanol-d_8 was also examined to further probe the possible involvement of an enolate complex during transfer hydrogenation with **2**. Under the same standard conditions as described above, the concentration of benzophenone was varied from 0.15−0.37 M. The reaction progress again follows a single exponential decay (Figures S25−S27); however, the rates do not exhibit substrate inhibition, and the observed rate constants k_{obs} are approximately independent of benzophenone concentration within experimental error (Figure S28).

Proposed Mechanism. On the basis of the experimental data on the transfer hydrogenation of ketones with **2**, a three-step mechanism for product formation is proposed with an additional off-path equilibrium, as shown in Scheme 4. The Ru−hydride **2** reacts with the ketone substrate[38] to generate a Ru−alkoxide intermediate (step A). Alkoxide exchange to form the Ru−isopropoxide complex and release the product alcohol is driven by the presence of a large excess of isopropanol solvent (step B). Regeneration of **2** occurs by elimination of acetone from the Ru−isopropoxide (step C). We recently reported an experimental and theoretical study of the energetics and mechanism for the reaction of ketones with **2**, which established that the Ru−hydride **2** reacts rapidly and reversibly with acetone to generate the Ru−isopropoxide (steps A and C) in a near-ergoneutral equilibrium process.[38]

The reversible formation of a Ru−enolate complex (step D) is proposed as an off-path equilibrium process responsible for the observed decrease in the rate of transfer hydrogenation with increasing 2-heptanone concentration. Previous studies have established the Ru−isopropoxide as the catalyst resting state in Scheme 4 when isopropanol is present in large excess.[44,45] Partial or full ionization of this Ru−O bond[44] would generate the isopropoxide anion that can deprotonate the ketone substrate to form the corresponding enolate, which may be stabilized via coordination to ruthenium.

The mechanism of transfer hydrogenation starting from the Ru−chloride precatalyst **1** is similar; however, an initial activation step with strong base is required to generate the active Ru−OR species.[41] Baratta and co-workers observed an increase in the rate of transfer hydrogenation with increasing sodium isopropoxide concentration up to 100 equiv relative to **1** in refluxing isopropanol,[44] although in our hands, the rate enhancement beyond 20 equiv of base is negligible at 25 °C. Notably, there is no rate improvement with the addition of base when using the Ru−hydride **2** as the preformed active catalyst (vide supra); therefore, the reversible formation of a cationic isopropanol complex suggested by Baratta is not included here.[44]

Electrochemical Studies. *Characterization.* The electrochemical properties of **1**−**3** are summarized in Table 3. All measurements were performed in tetrahydrofuran with tetra-*n*-butylammonium hexafluorophosphate as supporting electrolyte, unless otherwise noted. The Ru−chloride **1** exhibits a reversible one-electron oxidation at −0.20 V versus ferrocene/ferrocenium ($Fc^{0/+}$), which is assigned to the Ru^{II}/Ru^{III} couple (Figure 4a). The Ru−phenoxide **3** also displays a reversible Ru^{II}/Ru^{III} couple at a slightly more negative potential than **1** (Figure 4b). The large peak-to-peak separation for both features is attributed to uncompensated solution resistance in tetrahydrofuran (ε = 7.58 at 25 °C), as ferrocene displays a similarly large ΔE_p at the same scan rate (Figure S29).

The Ru−hydride **2** is oxidized at −0.80 V versus $Fc^{0/+}$ at 100 mV/s (Figure 4c), and the anodic peak current i_a shows a linear dependence on the concentration of **2** (Figure 4c, inset). This oxidation potential is significantly lower than the Ru^{II}/Ru^{III} couple of the chloride or phenoxide complexes **1** and **3**. The ordering of oxidation potentials in this series (i.e., **2** < **3** < **1**) scales with the basicity of the anionic ligand. Furthermore, this potential is lower than that observed for the oxidation of other neutral Ru−hydride complexes such as $[Cp^*RuH(PPh_3)_2]$[54] likely as a consequence of the strongly donating, anionic CNN

DOI: 10.1021/jacs.6b09705
J. Am. Chem. Soc. 2017, 139, 738−748

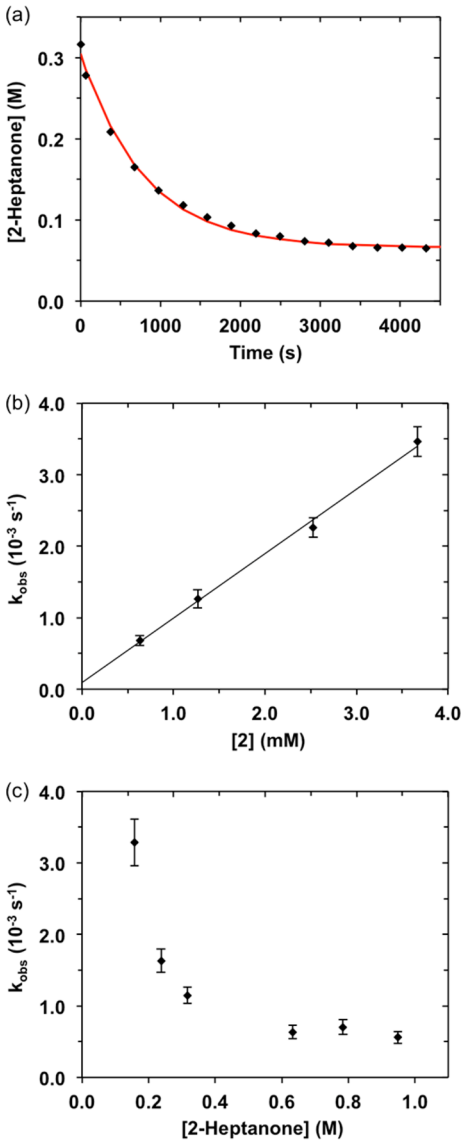

Figure 3. (a) Conversion of 2-heptanone over time for Table 2, entry 2: single exponential decay fit (red). (b) Dependence of k_{obs} on the concentration of the Ru–hydride **2**. (c) Dependence of k_{obs} on the concentration of 2-heptanone.

Scheme 3. Deuteration of 2-Heptanone during Transfer Hydrogenation with 2[a]

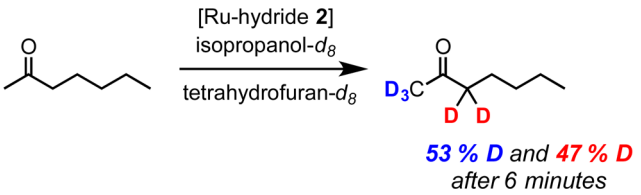

[a]Conditions: 1.26 mM **2**, 0.32 M 2-heptanone, 3.16 M isopropanol-d_8 in tetrahydrofuran-d_8.

ligand. The oxidation of **2** is chemically irreversible, and no discernible reduction feature is observed up to 2 V/s (Figure S29). This behavior is consistent with a fast chemical step occurring after initial oxidation of the Ru^{II}–hydride. In the presence of an equimolar solution of ferrocene, integration of the voltammagram reveals that the area of the Ru–hydride oxidation wave is approximately equal to that of the ferrocene oxidation wave (Figure S29), establishing this as a one-electron per ruthenium oxidation. Furthermore, the charge passed during a controlled-potential electrolysis of **2** at −0.60 V versus $Fc^{0/+}$ is 91% of the theoretical value for a one-electron process (Figure S43).

The oxidation of d^6 metal–hydrides is often followed by further complex reactions.[55−58] To determine the nature of the oxidation product, the Ru–hydride **2** was treated with ferrocenium tetrafluoroborate ($Fc^+BF_4^-$) as a one-electron chemical oxidant. The addition of 1 equiv of $Fc^+BF_4^-$ to a solution of **2** in tetrahydrofuran-d_8 resulted in complete conversion to a single Ru species, as observed by ^1H and ^{31}P NMR. Unexpectedly, the ^1H and ^{31}P NMR spectra of this product are identical to those of Ru–chloride **1** (Figures S37 and S38). Oxidation using perchlorate salts of silver(I) or ferrocenium also yielded similar NMR spectra. We tentatively assign this species as the six-coordinate complex [RuX(CNN)(dppb)] (X = ClO_4^- or BF_4^-), where either the perchlorate or the tetrafluoroborate anion is bound to the ruthenium center. The ability of these typically noncoordinating anions to function as ligands in transition metal complexes has been previously reported.[59−65] On the other hand, chemical oxidation of **2** with ferrocenium or silver(I) in acetonitrile leads to rapid formation of the cationic acetonitrile complex $[Ru(CH_3CN)(CNN)(dppb)]^+$ **4** as the major product based on ^1H and ^{31}P NMR analysis.[42] Formation of the [Ru–solvato] cation in acetonitrile versus the [Ru–X] complex in tetrahydrofuran is in line with the stronger ligating ability of acetonitrile. Furthermore, the formation of dihydrogen is observed by ^1H NMR analysis of the reaction (Figure S39), demonstrating that one-electron oxidation of **2** results in H_2 evolution.

Two reasonable mechanisms for the oxidation of the Ru–hydride **2** are depicted in Scheme 5: (a) one-electron oxidation to the Ru^{III}–hydride cation followed by deprotonation by another equivalent of Ru^{II}–hydride and rapid reoxidation of the transient Ru^I species ($E_rC_iE_r'$); or (b) one-electron oxidation to the Ru^{III}–hydride cation followed by bimolecular elimination of hydrogen ($E_rE_rC_i$). The overall stoichiometry for either mechanism is one-electron per ruthenium with the concomitant formation of dihydrogen, consistent with the results of our chemical oxidation experiments. While the data to date do not allow us to distinguish between the mechanisms in Scheme 5a and b for the oxidation of **2** in the absence of base, deprotonation of the Ru^{III}–hydride by solvent or electrolyte can be ruled out (Scheme 5c), as this would require an overall stoichiometry of two-electrons per ruthenium and would not produce H_2.

Treatment with Base. Treatment of the Ru–chloride **1** with alkoxides in the presence of excess alcohol generates the Ru alkoxides.[41] We note that it is critical that the alkoxide base be added to a solution of **1** only after the addition of alcohol; in the absence of isopropanol or other alcohol, treatment of **1** with alkoxide base (*t*-butoxide or isopropoxide) causes the solution color to immediately change from yellow to dark brown with the accompanying formation of an unidentified black precipitate. Cyclic voltammetry of the dark solution yields no discernible features within a potential window of −1 to +0.5 V versus $Fc^{0/+}$, indicating decomposition has occurred. In contrast, the Ru–hydride **2** is stable in the presence of potassium *t*-butoxide, even in the absence of alcohol: neither decomposition nor deprotonation of **2** occurs based on ^1H

DOI: 10.1021/jacs.6b09705
J. Am. Chem. Soc. 2017, 139, 738–748

Scheme 4. Proposed Mechanism for Ketone Transfer Hydrogenation with Isopropanol Using the Ru−Hydride 2

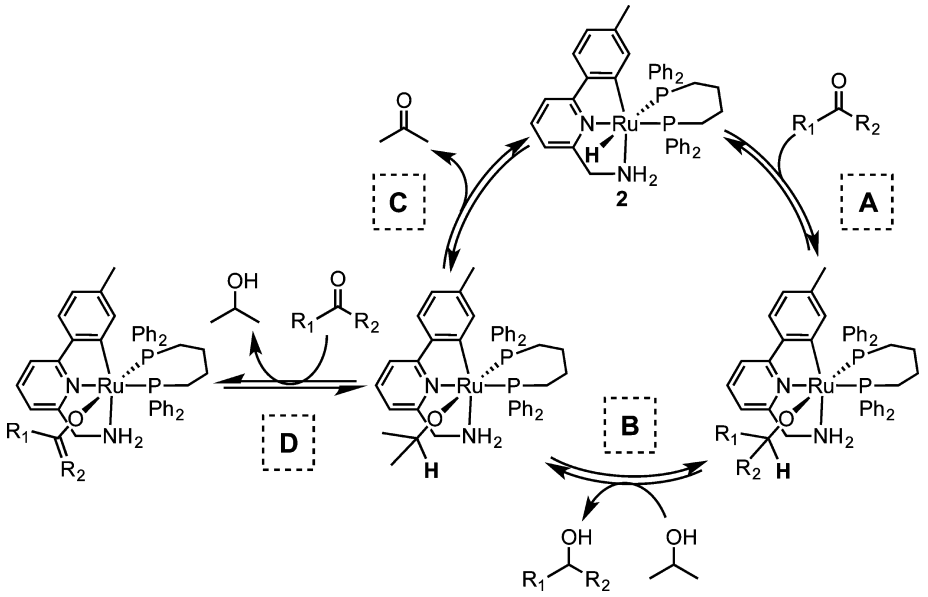

Table 3. Cyclic Voltammetry Data of 1−3[a]

complex	$E_{1/2}$ (V)[b]	ΔE_p (mV)[d]	i_a/i_c[e]
1	−0.20	155	1.01
2	−0.80[c]		
3	−0.35	235	1.08

[a]Conditions: 1 mM Ru in 0.1 M Bu_4NPF_6 in tetrahydrofuran, glassy carbon working electrode, Pt auxiliary electrode, $Ag/AgNO_3$ reference electrode, 100 mV/s. [b]$E_{1/2} = 0.5(E_{pa} + E_{pc})$, where E_{pa} and E_{pc} are anodic and cathodic peak potentials, respectively. Potentials reported versus $Fc^{0/+}$. [c]Oxidation potential of chemically irreversible feature. [d]$\Delta E_p = E_{pa} - E_{pc}$. [e]$i_a$ = andodic peak current, i_c = cathodic peak current.

NMR (Figure S40). By cyclic voltammetry, the addition of excess potassium *t*-butoxide (20 mM) to a solution of **2** (1 mM) results in a marked increase in the current of the one-electron oxidation at −0.80 V (Figure 5). Integration of the voltammogram before and after addition of base reveals that the area of the wave is doubled in the presence of potassium *t*-butoxide. Furthermore, controlled-potential electrolysis of **2** in the presence of 35 equiv of potassium *t*-butoxide is consistent with an overall two-electron oxidation (Figure S44). These results imply that rapid deprotonation of the Ru^{III}−hydride cation by alkoxide base occurs after one-electron oxidation of **2**, generating a transient Ru^{I} species that would be rapidly oxidized by the electrode at these potentials (Scheme 5c).[66] Therefore, the oxidation of **2** in the presence of potassium *t*-butoxide is an overall two-electron-one-proton process according to mechanism (c) shown in Scheme 5. Amines such as 1,4-diazabicyclo[2.2.2]octane (DABCO) and 1,5,7-triazabicyclo[4.4.0]dec-5-ene (TBD) do not affect the electrochemical behavior of **2**, indicating that these bases are not sufficiently strong to change the mechanism of Ru−hydride oxidation from a one-electron to two-electron per ruthenium process.

Electrocatalytic Alcohol Oxidation. The two-electron-one-proton oxidation of the Ru−hydride **2** in the presence of potassium *t*-butoxide represents the key electrochemical step for the electrocatalytic oxidation of alcohols, as proposed in Figure 1. Following two-electron-one-proton oxidation of **2**, formation of a cationic Ru−isopropanol intermediate is expected to proceed rapidly in alcohol solution, and deprotonation to the Ru−isopropoxide complex should occur under sufficiently basic conditions.[45] Regeneration of **2** from the Ru−isopropoxide would close the electrocatalytic cycle (Scheme 6). In fact, an increase in current of the low-potential oxidation for **2** in the presence of isopropanol (Figure S33) suggests that such an electrocatalytic cycle for isopropanol oxidation may be operative even in the absence of base.[67]

Further studies into the electrocatalytic oxidation of isopropanol were performed using the Ru−chloride precatalyst **1**. We note that potassium *t*-butoxide was added to electrochemical solutions of **1** only following the addition of isopropanol to avoid decomposition of the complex. At low concentrations of potassium *t*-butoxide with a large excess of isopropanol (0.5 M), the conversion of **1** into the Ru−hydride and Ru−isopropoxide complexes is evident by cyclic voltammetry (Figure 6). The oxidation feature at −0.4 V versus $Fc^{0/+}$ is assigned to oxidation of the Ru−isopropoxide complex based on comparison to the redox potential of the Ru−phenoxide **3**. This behavior mirrors the results from chemical transfer hydrogenation studies where treatment of the Ru−chloride **1** with base and alcohol yields a mixture of the hydride and alkoxide species under ambient conditions. Further addition of potassium *t*-butoxide results in a significant increase in current at an onset potential near that of the Ru−hydride oxidation and reaching a maximum current at ca. −0.5 V versus $Fc^{0/+}$ (Figure 7a).

To determine the origin of the electrocatalytic current, controlled potential electrolysis of **1** in the presence of isopropanol and potassium *t*-butoxide was performed at −0.6 V versus $Fc^{0/+}$ (Figure S45). A higher electrolyte concentration (0.2 M) in 1:1 tetrahydrofuran/1,2-difluorobenzene was used here to decrease the resistivity of the solution. Analysis of the working electrode compartment solution postelectrolysis by gas chromatography reveals acetone to be the two-electron oxidation product, generated with a Faradaic efficiency of 94 ± 5%. No acetone is produced in the absence of applied potential. Furthermore, for the controlled potential electrolysis in the absence of **1** under otherwise identical conditions, the

DOI: 10.1021/jacs.6b09705
J. Am. Chem. Soc. 2017, 139, 738−748

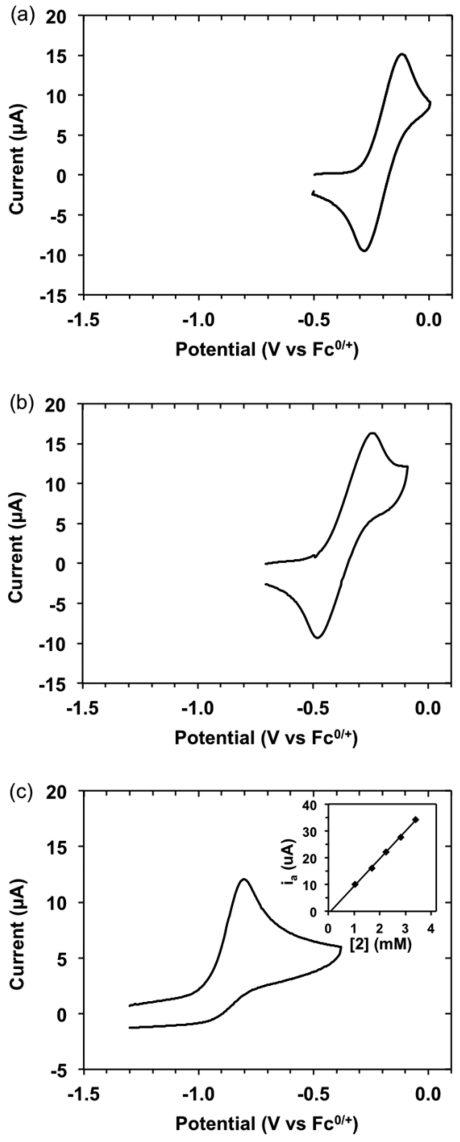

Figure 4. Cyclic voltammograms of (a) Ru–chloride **1**, (b) Ru–phenoxide **3**, and (c) Ru–hydride **2** (1 mM Ru in 0.1 M Bu_4NPF_6) in tetrahydrofuran. Scan rate 100 mV/s. Inset: Dependence of the oxidative peak current i_a on [**2**].

current decays to background levels rapidly (Figure S46), indicating that oxidation of isopropanol at the carbon working electrode is negligible at this potential.

The catalytic turnover frequency (TOF) for the electrocatalytic oxidation of isopropanol can be roughly estimated from the catalytic current enhancement i_{cat}/i_p, the ratio of the maximum catalytic current i_{cat} to the peak current i_p in the absence of substrate. Using eqs 1 and 2 for i_{cat} and i_p, respectively, eq 3 for i_{cat}/i_p is derived,[68−71] where n_{cat} is the number of electrons consumed in the catalytic reaction, n_p is the number of electrons transferred in the absence of substrate, F is Faraday's constant, A is electrode area, D is diffusion coefficient, R is universal gas constant, T is temperature, v is scan rate (V/s), and k_{obs} is the pseudo first-order rate constant:

$$i_{cat} = n_{cat}FA[\text{catalyst}]\sqrt{Dk_{obs}} \quad (1)$$

Scheme 5. Possible Mechanisms for the Electrochemical Oxidation of the Ru–Hydride 2[a]

(a)
$$Ru^{II}–H \longrightarrow Ru^{III}–H^{+} + e^{-}$$
$$Ru^{III}–H^{+} + Ru^{II}–H \longrightarrow Ru^{I} + Ru^{II}–X^{n+} + H_2$$
$$Ru^{I} \longrightarrow Ru^{II}–X^{n+} + e^{-}$$

(b)
$$Ru^{II}–H \longrightarrow Ru^{III}–H^{+} + e^{-}$$
$$2\,Ru^{III}–H^{+} \longrightarrow 2\,Ru^{II}–X^{n+} + H_2$$

(c)
$$Ru^{II}–H \longrightarrow Ru^{III}–H^{+} + e^{-}$$
$$Ru^{III}–H^{+} \longrightarrow Ru^{I} + H^{+}$$
$$Ru^{I} \longrightarrow Ru^{II}–X^{n+} + e^{-}$$

[a]Where X = solvent (n = 1) or electrolyte anion (n = 0).

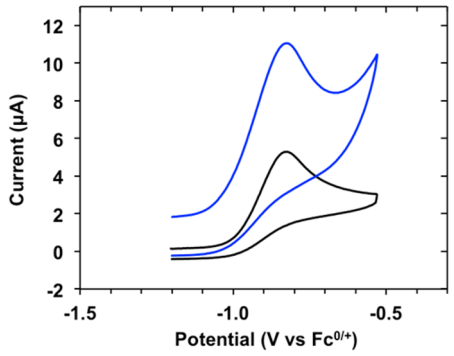

Figure 5. Cyclic voltammograms of the Ru–hydride **2** (1 mM Ru in 0.1 M Bu_4NPF_6) in tetrahydrofuran without base (black), and with 20 mM potassium *t*-butoxide (blue). Scan rate 25 mV/s.

$$i_p = 0.4463\left(\frac{F^3}{RT}\right)^{1/2} n_p^{3/2} AD^{1/2}[\text{catalyst}]v^{1/2} \quad (2)$$

$$\frac{i_{cat}}{i_p} = \frac{n_{cat}}{0.4463}\sqrt{\frac{RTk_{obs}}{Fvn_p^3}} \quad (3)$$

For a plateau-shaped wave under substrate saturation conditions, the TOF is related to the pseudo first-order rate constant k_{obs}. Using eq 3, the turnover frequency for the two-electron oxidation of isopropanol to acetone with **1** is thus estimated to be 3.2 s^{-1}. While this method of determining the rate constant is approximate,[72] the calculated k_{obs} value is in reasonable agreement with the TOF observed for the chemical transfer hydrogenation of acetophenone with **1** in isopropanol at 25 °C (ca. 1 s^{-1}). Electrocatalytic current is also observed starting with the Ru–hydride **2** under the same conditions (Figure S36). Unexpectedly, a higher TOF (4.8 s^{-1}) for isopropoxide oxidation is estimated for the Ru–hydride **2** as compared to the Ru–chloride **1**. The origin of this rate difference is not clear, although it may be attributed to incomplete activation of the Ru–chloride precatalyst.

There are limited examples of transition metal complexes beyond the Ru poly pyridyl oxo systems[30−32] that are capable of electrocatalytic alcohol oxidation. Oxidation of 4-methoxybenzyl alcohol to the corresponding aldehyde with Ir-diamino-

DOI: 10.1021/jacs.6b09705
J. Am. Chem. Soc. 2017, 139, 738−748

Scheme 6. Proposed Mechanism for the Electrocatalytic Oxidation of Isopropanol in Tetrahydrofuran

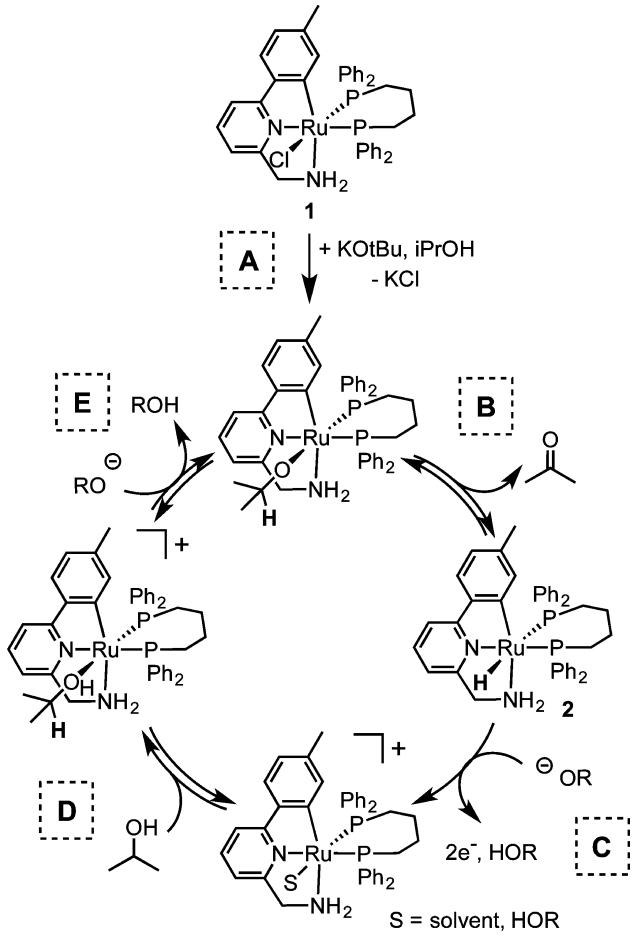

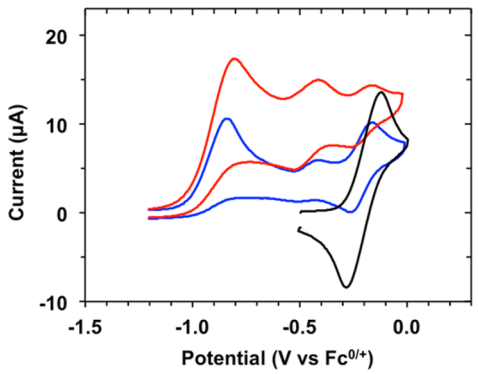

Figure 6. Cyclic voltammograms of the Ru–chloride **1** (1 mM Ru) in tetrahydrofuran with 0.5 M isopropanol (black), followed by addition of 1 mM (blue) and 2 mM (red) potassium *t*-butoxide. Scan rate 100 mV/s.

diolefin catalysts in the presence of sodium 4-nonylphenolate occurs at −0.06 V versus $Fc^{0/+}$ in *ortho*-dichlorobenzene,[73] or using ferrocenium as a chemical oxidant.[74] An "organometallic fuel cell" for the electrocatalytic oxidation of ethanol to acetate was constructed using a Rh–hydride catalyst in aqueous KOH solution.[75,76] Appel and co-workers[70] reported the oxidation of isopropanol using a Ni phosphine catalyst bearing pendant amines at −0.4 V versus $Fc^{0/+}$ in acetonitrile with triethylamine as the base. Recently, the electrocatalytic oxidation of a series of alcohols at −0.14 V versus $Fc^{0/+}$ was achieved using a Cu^{I}/nitroxyl radical cocatalyst with triethylamine in acetonitrile.[77] The TOF for isopropanol oxidation with this Cu^{I}/nitroxyl system is ca. 3 s^{-1}, comparable to that exhibited by ruthenium complexes **1** and **2**, while the TOF of the Ni catalyst[70] is approximately 7 times lower. Direct comparison of the catalytic activity and overpotentials of these catalyst systems is complicated due to the use of different solvents and ill-defined pH in nonaqueous solution; however, we note that the overpotential for electrocatalysis with **1** and **2** is likely considerably larger than that of the Ni and Cu systems due to the difference in the strength of the base required for electrocatalysis. There is an ca. 21 unit difference between the pK_a's of triethylammonium and isopropanol, which correlates to a significant (1.2 V) difference in the equilibrium potential E_0 for the isopropanol/acetone couple.

The effects of the base, alcohol, and catalyst on the electrocatalytic behavior of **1** were examined by varying the concentration of each component individually. As seen in Figure 7b, the catalytic current i_{cat} shows a linear correlation to the concentration of the Ru–chloride **1** between 0.5–1.8 mM, indicating a first-order dependence on [**1**] according to eq 1. The TOF increases linearly with isopropanol concentration up to 0.5 M (Figure S34), after which point the current becomes independent of alcohol, indicative of saturation behavior. There is a second-order dependence of the catalytic current on the concentration of potassium *t*-butoxide up to 6–8 mM, and no further rate increase is observed at higher base concentrations (Figure S35). This behavior is attributed to activation of the Ru–chloride **1**, which is known from transfer hydrogenation studies to be slow in the absence of a large excess of alkoxide (vide supra).

A proposed mechanism for the electrocatalytic oxidation of isopropanol is depicted in Scheme 6. In the presence of excess isopropanol and isopropoxide base, the Ru–chloride precatalyst **1** is activated via elimination of potassium chloride and formation of the Ru–isopropoxide complex (step A). It is well established from the known transfer hydrogenation and chemical reactivity studies with this system that the reversible interconversion between the Ru–isopropoxide complex and the Ru–hydride **2** is rapid and near ergoneutral under ambient conditions.[38] Thus, generation of Ru–hydride **2** with concomitant release of acetone in step B is facile. Electrochemical oxidation of **2** at ca. −0.8 V versus $Fc^{0/+}$ occurs via an overall two-electron one-proton process under basic conditions, generating a Ru^{II} cationic complex that may be stabilized by an electrolyte anion or solvent at the sixth coordination site (step C). With a large excess of isopropanol in solution, the cationic Ru–isopropanol complex will readily form via coordination of isopropanol (step D). The rapid coordination of alcohols to complexes of this type has been previously demonstrated.[45] Finally, the Ru–isopropoxide complex is regenerated by deprotonation of the Ru–isopropanol species in the presence of sufficiently strong base (step E).[45]

CONCLUSIONS

The octahedral Ru–chloride and hydride complexes **1** and **2** are highly active for ketone transfer hydrogenation under ambient conditions, displaying TOFs of ca. 1 s^{-1} when isopropanol is used as the hydrogen donor. Kinetic studies probing the mechanism of 2-heptanone transfer hydrogenation with **2** are indicative of substrate inhibition at higher ketone concentrations. Under electrochemical conditions in the absence of ketone substrate, **1** and **2** are both active for

DOI: 10.1021/jacs.6b09705
J. Am. Chem. Soc. 2017, 139, 738–748

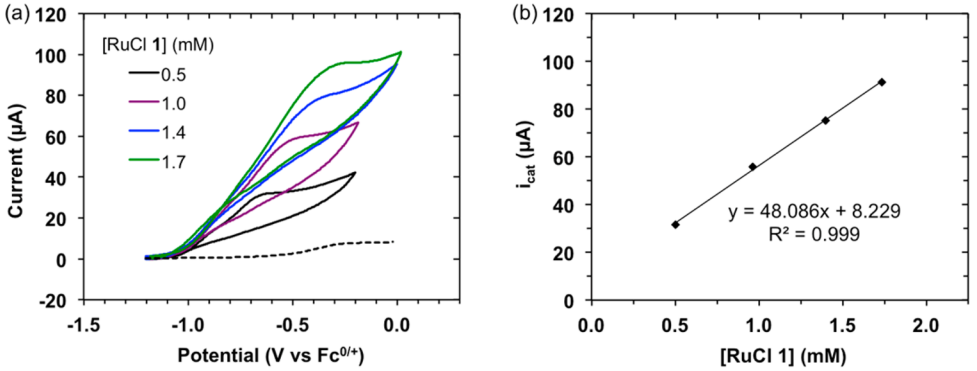

Figure 7. (a) Cyclic voltammograms of the Ru−chloride **1** (0.5 mM Ru) with isopropanol (0.5 M) and potassium *t*-butoxide (23 mM) in tetrahydrofuran (black, solid), followed by further addition of **1**. Cyclic voltammogram of isopropanol (0.5 M) and potassium *t*-butoxide (23 mM) in the absence of **1** shown by black dashed trace. Scan rate 100 mV/s. (b) [**1**] dependence on the maximum catalytic current i_{cat}.

electrocatalytic isopropanol oxidation in the presence of alkoxide base. The Ru−chloride **1** exhibits a rate of 3.2 s^{-1} for isopropanol electrooxidation at ca. −0.6 V versus $Fc^{0/+}$, while a turnover frequency of 4.8 s^{-1} is achieved using the Ru−hydride **2**. The onset potential for electrooxidation occurs near that of the oxidation of **2**, suggesting that the two-electron, one-proton oxidation of the Ru−hydride complex is a critical step in the electrocatalytic mechanism. Controlled potential electrolysis establishes acetone as the product of the two-electron oxidation of isopropanol. This work demonstrates the promising utility of transfer hydrogenation catalysts for the discovery of new alcohol electrooxidation systems based on reactive metal hydrides.

EXPERIMENTAL SECTION

Materials. All manipulations were carried out under an inert atmosphere of nitrogen or argon with the use of standard vacuum line, Schlenk, and glovebox techniques. Solvents were dried by standard methods and degassed via three freeze−pump−thaw cycles. Deuterated solvents for NMR were purchased from Cambridge Isotope Laboratories. All reagents were used as received unless otherwise described. The syntheses of the Ru−chloride **1**[39] and Ru−hydride **2**[38] were described previously. Benzophenone (Sigma-Aldrich) was purified by sublimation prior to use. Tetrabutylammonium hexafluorophosphate (Sigma-Aldrich) was recrystallized from ethanol, dried under reduced pressure, and stored in an inert atmosphere glovebox. Ferrocene (Sigma-Aldrich) was sublimed under vacuum, and stored in an inert atmosphere glovebox.

Instrumentation. NMR spectra were recorded on Varian 300, 500, or 600 MHz spectrometers. All NMR spectra were taken at room temperature unless stated otherwise. Residual solvent proton and carbon peaks were used as reference. Chemical shifts are reported in parts per million (δ). High-resolution mass spectra were obtained by LC/ESI−MS on a Waters Acquity UPLC and Thermo Fisher Exactive Orbitrap mass spectrometer. CHN elemental analysis was performed by Robertson Microlit Laboratories, NJ.

Single crystals for X-ray analysis were mounted on a Kapton loop using Paratone N hydrocarbon oil. Measurements were made on a Bruker Kappa X8-APEX II diffractometer with graphite monochromated Mo Kα radiation (λ = 0.71073 Å). Frames corresponding to an arbitrary sphere of data were collected using a combination of ω- and φ-scans of 0.5°. Data were corrected for absorption and polarization effects, and analyzed for space group determination. Structures were solved by direct methods,[78] expanded routinely, and refined by full-matrix least-squares procedures based on F^2.[79] Hydrogen atoms were included in ideal positions and refined isotropically in riding model with $U_{iso} = 1.5U_{eq}(X)$ for methyl groups and $U_{iso} = 1.2U_{eq}(X)$ for other atoms, where $U_{eq}(X)$ are thermal parameters of parent atoms. Non-hydrogen atoms were refined anisotropically. Crystallographic data for **3** are presented in the Supporting Information.

Cyclic voltammetry experiments were performed using a WaveNow USB potentiostat (Pine Research Instrumentation) at ambient temperature in an inert atmosphere glovebox. A typical electrochemical cell consisted of a three-electrode setup using a glassy carbon working electrode (3 mm diameter, Bioanalytical Systems, Inc.), platinum wire auxiliary electrode, and $Ag/AgNO_3$ nonaqueous reference electrode (Bioanalytical Systems, Inc.). All electrochemical experiments were performed with 0.1 M tetrabutylammonium hexafluorophosphate supporting electrolyte in tetrahydrofuran, unless stated otherwise. No compensation for the solution resistance was applied in any cyclic voltammetry experiments. The glassy carbon working electrode was polished between each scan. Potentials are referenced to the $Fc^{0/+}$ couple (0.0 V) using cobaltocenium hexafluorophosphate (−1.3 V) as an internal reference.

Controlled potential electrolysis was performed using a standard two-compartment H-cell, or custom gastight cell (see Supporting Information) with a Teflon cap having openings customized to accept each electrode or cell component: glassy carbon disk (3 mm diameter, Bioanalytical Systems) for cyclic voltammetry, carbon cloth (Fuel Cell Store) for electrolysis, and $Ag/AgNO_3$ nonaqueous reference electrode (Bioanalytical Systems, Inc.) isolated from the solution by a Vycor frit. A platinum coil was used as the auxiliary electrode, which was separated from the cell solution in a 12 mm diameter glass tube terminating with a 20 mm diameter fine glass frit. Acetone was quantified using a Shimadzu GC-2014 gas chromatograph equipped with a thermal conductivity detector, a CarbonPLOT column, and nitrogen carrier gas. Faradaic efficiency is given by comparing the total product formation to the theoretical amount based on the charge passed during electrolysis.

Synthesis. *[Ru(OC$_6$H$_5$)(CNN)(dppb)]* ***3***. Potassium *t*-butoxide (0.023 g, 0.20 mmol) was added to a solution of the Ru−chloride **1** (0.15 g, 0.20 mmol) and phenol (0.024 g, 0.25 mmol) in tetrahydrofuran (20 mL). The solution was stirred at room temperature for 4.5 h, and then filtered through a Celite plug. The resulting filtrate was evaporated in vacuo to yield **3** as an orange powder. Yield 85% (0.14 g). X-ray quality crystals were obtained by slow evaporation of a solution of **3** in *p*-xylene. ^{1}H NMR (500 MHz, C_6D_6) δ 8.57 (t, J = 8.5 Hz, 2H), 8.02 (t, J = 7.6 Hz, 2H), 7.82 (s, 1H), 7.38 (br s, 2H), 7.29−7.25 (m, 3H), 7.20 (d, J = 7.2 Hz, 2H), 7.16−7.08 (m, 5H), 7.01 (dd, J = 7.7, 0.9 Hz, 1H), 6.96 (dd, J = 8.4, 7.2 Hz, 2H), 6.63 (t, J = 7.3 Hz, 1H), 6.53 (t, J = 7.8 Hz, 2H), 6.47 (br m, 2H), 6.42 (t, J = 7.8 Hz, 1H), 6.23 (d, J = 7.5 Hz, 2H), 6.08 (br m, 2H), 5.81 (d, J = 7.4 Hz, 1H), 4.55 (br m, 1H), 3.28 (dd, J = 15.3, 4.1 Hz, 1H), 3.17−3.12 (m, 1H), 3.06 (q, J = 12.8 Hz, 1H), 3.00 (t, J = 13.2 Hz, 1H), 2.31 (s, 3H), 2.12 (dd, J = 14.6, 9.2 Hz, 1H), 2.03 (t, J = 14.4 Hz, 1H), 1.91−1.66 (m, 4H), 0.96−0.93 (m, 1H). ^{13}C NMR (125 MHz, C_6D_6) δ 184.8, 168.5, 163.9, 156.3, 148.9 (d, J = 2.6 Hz), 148.3 (d, J = 1.1 Hz), 144.3 (d, J = 30.0 Hz), 140.8 (d, J = 30.0 Hz), 138.1 (d, J = 29.2 Hz), 136.1, 135.6 (d, J = 10.8 Hz), 135.4 (d, J = 29.5 Hz),

DOI: 10.1021/jacs.6b09705
J. Am. Chem. Soc. 2017, 139, 738−748

134.3, 133.8, 131.3 (d, J = 7.1 Hz), 130.0 (d, J = 7.8 Hz), 129.4 (d, J = 25.9 Hz), 126.8, 126.3 (d, J = 7.8 Hz), 123.0, 121.6, 121.1, 115.3, 114.9, 112.8, 51.9, 31.1 (d, J = 27.9 Hz), 30.6 (d, J = 25.2 Hz), 26.8, 22.1, 22.0. ^{31}P NMR (162 MHz, C_6D_6) δ 61.2 (d, J = 35.1 Hz), 39.4 (d, J = 35.1 Hz). Anal. Calcd for $C_{54}H_{54}N_2OP_2Ru$ [M + C_7H_8]: C, 71.27; H, 5.98; N, 3.08. Found: C, 71.23; H, 5.64; N, 3.45. HRMS calcd for $C_{41}H_{41}N_2P_2Ru$ [$(M - OC_6H_5)^+$]: m/z 725.1788. Found: m/z 725.1789.

Chemical Studies. *Representative Procedure for Turnover Frequency Measurement.* A stock solution of **1** (0.019 M) was prepared in tetrahydrofuran-d_8, and a 25 μL aliquot was added to a sealable NMR tube in an inert atmosphere glovebox. A stock solution of acetophenone (1.26 M), isopropanol (7.51 M), and the internal standard p-xylene (1.26 M) was prepared in tetrahydrofuran-d_8, and a 0.4 mL aliquot was added via syringe to the NMR tube. A stock solution of potassium t-butoxide (0.067 M) in tetrahydrofuran-d_8 was prepared, and a 0.175 mL aliquot was added to the NMR tube via syringe to initiate the reaction. The initial turnover frequency was determined by ^{1}H NMR from the conversion of acetophenone after 15 min according to the following equation:

$$\text{TOF} = \frac{\text{mmol of acetophenone consumed}}{(\text{mmol of catalyst})(\text{time})}$$

Representative Procedure for Transfer Hydrogenation Kinetics. In a typical experiment, Ru−hydride **2** (1.0 mg, 0.0014 mmol) was weighed into a sealable NMR tube in an inert atmosphere glovebox. A solution of 2-heptanone (48 μL, 0.34 mmol), isopropanol-d_8 (262 μL, 3.42 mmol), and the internal standard p-xylene (39 μL, 0.32 mmol) was prepared in tetrahydrofuran-d_8 (0.74 mL), and was added via syringe to the NMR tube. The reaction progress was monitored by ^{1}H NMR, and pseudo-first-order rate constants k_{obs} were obtained by fitting [2-heptanone] versus time to a single exponential decay, with R^2 > 0.99. Plots showing ketone conversion over time and pseudo-first-order fits are given in the Supporting Information.

Representative Procedure for Chemical Oxidation of Ru Complexes. Ru−hydride **2** (2.9 mg, 0.004 mmol) was weighed into a sealable NMR tube and dissolved in tetrahydrofuran-d_8 (0.6 mL) in an inert atmosphere glovebox. Ferrocenium tetrafluoroborate (1.1 mg, 0.004 mmol) was added, and the resulting mixture was analyzed by ^{1}H and ^{31}P NMR to establish the identity of the oxidation products.

■ ASSOCIATED CONTENT

Supporting Information

The Supporting Information is available free of charge on the ACS Publications website at DOI: 10.1021/jacs.6b09705.

Tabulated X-ray data, and molecular structures obtained from single crystal X-ray diffraction; ^{1}H NMR spectrum of **3**; conversion versus time plots for transfer hydrogenation kinetic studies; and additional cyclic voltammograms, chemical oxidation studies, and controlled potential electrolysis plots (PDF)

X-ray crystallographic data for compound **3** (CIF)

■ AUTHOR INFORMATION

Corresponding Author

*waymouth@stanford.edu

ORCID

Elizabeth McLoughlin: 0000-0003-1481-266X

Notes

The authors declare no competing financial interest.

■ ACKNOWLEDGMENTS

This material is based on work supported by the Global Climate and Energy Program at Stanford, and the National Science Foundation (CHE-1213403 and CHE-1565947). K.M.W. and K.R.F. are grateful for Center for Molecular Analysis and Design (CMAD) Fellowships. K.M.W. is also grateful for a Gabilan Stanford Graduate Fellowship and a National Science and Engineering Research Council of Canada (NSERC) Postgraduate Scholarship.

■ REFERENCES

(1) Gurau, B.; Viswanathan, R.; Liu, R.; Lafrenz, T. J.; Ley, K. L.; Smotkin, E. S.; Reddington, E.; Sapienza, A.; Chan, B. C.; Mallouk, T. E.; Sarangapani, S. *J. Phys. Chem. B* **1998**, *102*, 9997−10003.

(2) Liu, H.; Song, C.; Zhang, L.; Zhang, J.; Wang, H.; Wilkinson, D. P. *J. Power Sources* **2006**, *155*, 95−110.

(3) Bianchini, C.; Shen, P. K. *Chem. Rev.* **2009**, *109*, 4183−4206.

(4) Olah, G. A. *Angew. Chem., Int. Ed.* **2005**, *44*, 2636−2639.

(5) Joó, F. *ChemSusChem* **2008**, *1*, 805−808.

(6) Benson, E. E.; Kubiak, C. P.; Sathrum, A. J.; Smieja, J. M. *Chem. Soc. Rev.* **2009**, *38*, 89−99.

(7) DuBois, M. R.; DuBois, D. L. *Acc. Chem. Res.* **2009**, *42*, 1974−1982.

(8) Appel, A. M.; Bercaw, J. E.; Bocarsly, A. B.; Dobbek, H.; DuBois, D. L.; Dupuis, M.; Ferry, J. G.; Fujita, E.; Hille, R.; Kenis, P. J. A.; Kerfeld, C. A.; Morris, R. H.; Peden, C. H. F.; Portis, A. R.; Ragsdale, S. W.; Rauchfuss, T. B.; Reek, J. N. H.; Seefeldt, L. C.; Thauer, R. K.; Waldrop, G. L. *Chem. Rev.* **2013**, *113*, 6621−6658.

(9) Costentin, C.; Robert, M.; Savéant, J.-M. *Chem. Soc. Rev.* **2013**, *42*, 2423−2436.

(10) Darensbourg, D. J.; Rokicki, A.; Darensbourg, M. Y. *J. Am. Chem. Soc.* **1981**, *103*, 3223−3224.

(11) DuBois, D. L.; Berning, D. E. *Appl. Organomet. Chem.* **2000**, *14*, 860−862.

(12) Hayashi, H.; Ogo, S.; Abura, T.; Fukuzumi, S. *J. Am. Chem. Soc.* **2003**, *125*, 14266−14267.

(13) Jessop, P. G.; Joó, F.; Tai, C.-C. *Coord. Chem. Rev.* **2004**, *248*, 2425−2442.

(14) Creutz, C.; Chou, M. H. *J. Am. Chem. Soc.* **2007**, *129*, 10108−10109.

(15) Tanaka, R.; Yamashita, M.; Nozaki, K. *J. Am. Chem. Soc.* **2009**, *131*, 14168−14169.

(16) Federsel, C.; Boddien, A.; Jackstell, R.; Jennerjahn, R.; Dyson, P. J.; Scopelliti, R.; Laurenczy, G.; Beller, M. *Angew. Chem., Int. Ed.* **2010**, *49*, 9777−9780.

(17) Chakraborty, S.; Zhang, J.; Krause, J. A.; Guan, H. *J. Am. Chem. Soc.* **2010**, *132*, 8872−8873.

(18) Rankin, M. A.; Cummins, C. C. *J. Am. Chem. Soc.* **2010**, *132*, 10021−10023.

(19) Langer, R.; Diskin-Posner, Y.; Leitus, G.; Shimon, L. J. W.; Ben-David, Y.; Milstein, D. *Angew. Chem., Int. Ed.* **2011**, *50*, 9948−9952.

(20) Huff, C. A.; Sanford, M. S. *J. Am. Chem. Soc.* **2011**, *133*, 18122−18125.

(21) Tanaka, R.; Yamashita, M.; Chung, L. W.; Morokuma, K.; Nozaki, K. *Organometallics* **2011**, *30*, 6742−6750.

(22) Schmeier, T. J.; Dobereiner, G. E.; Crabtree, R. H.; Hazari, N. *J. Am. Chem. Soc.* **2011**, *133*, 9274−9277.

(23) Huff, C. A.; Sanford, M. S. *ACS Catal.* **2013**, *3*, 2412−2416.

(24) Zhang, Y.; MacIntosh, A. D.; Wong, J. L.; Bielinski, E. A.; Williard, P. G.; Mercado, B. Q.; Hazari, N.; Bernskoetter, W. H. *Chem. Sci.* **2015**, *6*, 4291−4299.

(25) Pugh, J. R.; Bruce, M. R. M.; Sullivan, B. P.; Meyer, T. J. *Inorg. Chem.* **1991**, *30*, 86−91.

(26) Kang, P.; Cheng, C.; Chen, Z.; Schauer, C. K.; Meyer, T. J.; Brookhart, M. *J. Am. Chem. Soc.* **2012**, *134*, 5500−5503.

(27) U.S. Energy Information Administration Consumption & Efficiency. *Monthly Energy Review, December 2015*; published online 2015; http://www.eia.gov/consumption/.

(28) U.S. Department of Energy, Energy Efficiency & Renewable Energy. *Alternative Fuels Data Center - Hydrogen*; published online 2014; http://www.afdc.energy.gov/fuels/hydrogen.html.

DOI: 10.1021/jacs.6b09705
J. Am. Chem. Soc. 2017, 139, 738−748

(29) Kakati, N.; Maiti, J.; Lee, S. H.; Jee, S. H.; Viswanathan, B.; Yoon, Y. S. *Chem. Rev.* **2014**, *114*, 12397−12429.
(30) Meyer, T. J.; Huynh, M. H. V. *Inorg. Chem.* **2003**, *42*, 8140−8160.
(31) Cheung, K.-C.; Wong, W.-L.; Ma, D.-L.; Lai, T.-S.; Wong, K.-Y. *Coord. Chem. Rev.* **2007**, *251*, 2367−2385.
(32) Paul, A.; Hull, J. F.; Norris, M. R.; Chen, Z.; Ess, D. H.; Concepcion, J. J.; Meyer, T. J. *Inorg. Chem.* **2011**, *50*, 1167−1169.
(33) Ikariya, T.; Blacker, A. J. *Acc. Chem. Res.* **2007**, *40*, 1300−1308.
(34) Palmer, M.; Walsgrove, T.; Wills, M. *J. Org. Chem.* **1997**, *62*, 5226−5228.
(35) Brownell, K. R. Ph.D. Thesis, Stanford University, 2012.
(36) Brownell, K. R.; McCrory, C. C. L.; Chidsey, C. E. D.; Perry, R. H.; Zare, R. N.; Waymouth, R. M. *J. Am. Chem. Soc.* **2013**, *135*, 14299−14305.
(37) Buonaiuto, M.; De Crisci, A. G.; Jaramillo, T. F.; Waymouth, R. M. *ACS Catal.* **2015**, *5*, 7343−7349.
(38) Ramakrishnan, S.; Waldie, K. M.; Warnke, I.; De Crisci, A. G.; Batista, V. S.; Waymouth, R. M.; Chidsey, C. E. D. *Inorg. Chem.* **2016**, *55*, 1623−1632.
(39) Baratta, W.; Chelucci, G.; Gladiali, S.; Siega, K.; Toniutti, M.; Zanette, M.; Zangrando, E.; Rigo, P. *Angew. Chem., Int. Ed.* **2005**, *44*, 6214−6219.
(40) Chelucci, G.; Baldino, S.; Baratta, W. *Coord. Chem. Rev.* **2015**, *300*, 29−85.
(41) Baratta, W.; Bosco, M.; Chelucci, G.; Zotto, A. D.; Siega, K.; Toniutti, M.; Zangrando, E.; Rigo, P. *Organometallics* **2006**, *25*, 4611−4620.
(42) Baratta, W.; Ballico, M.; Del Zotto, A.; Herdtweck, E.; Magnolia, S.; Peloso, R.; Siega, K.; Toniutti, M.; Zangrando, E.; Rigo, P. *Organometallics* **2009**, *28*, 4421−4430.
(43) Baratta, W.; Baldino, S.; Calhorda, M. J.; Costa, P. J.; Esposito, G.; Herdtweck, E.; Magnolia, S.; Mealli, C.; Messaoudi, A.; Mason, S. A.; Veiros, L. F. *Chem. - Eur. J.* **2014**, *20*, 13603−13617.
(44) Baratta, W.; Siega, K.; Rigo, P. *Chem. - Eur. J.* **2007**, *13*, 7479−7486.
(45) Baratta, W.; Ballico, M.; Esposito, G.; Rigo, P. *Chem. - Eur. J.* **2008**, *14*, 5588−5595.
(46) Friedrich, A.; Schneider, S. *ChemCatChem* **2009**, *1*, 72−73.
(47) Nielsen, M.; Kammer, A.; Cozzula, D.; Junge, H.; Gladiali, S.; Beller, M. *Angew. Chem., Int. Ed.* **2011**, *50*, 9593−9597.
(48) Baratta, W.; Bossi, G.; Putignano, E.; Rigo, P. *Chem. - Eur. J.* **2011**, *17*, 3474−3481.
(49) Wisman, R. V.; de Vries, J. G.; Deelman, B.-J.; Heeres, H. J. *Org. Process Res. Dev.* **2006**, *10*, 423−429.
(50) Rautenstrauch, V.; Hoang-Cong, X.; Churlaud, R.; Abdur-Rashid, K.; Morris, R. H. *Chem. - Eur. J.* **2003**, *9*, 4954−4967.
(51) Wylie, W. N. O.; Lough, A. J.; Morris, R. H. *Organometallics* **2011**, *30*, 1236−1252.
(52) Mikhailine, A. A.; Maishan, M. I.; Lough, A. J.; Morris, R. H. *J. Am. Chem. Soc.* **2012**, *134*, 12266−12280.
(53) Bossi, G.; Putignano, E.; Rigo, P.; Baratta, W. *Dalton Trans.* **2011**, *40*, 8986−8995.
(54) Romming, C.; Smith, K.-T.; Tilset, M. *Inorg. Chim. Acta* **1997**, *259*, 281−290.
(55) Smith, K.-T.; Ramming, C.; Tilset, M. *J. Am. Chem. Soc.* **1993**, *115*, 8681−8689.
(56) Bianchini, C.; Peruzzini, M.; Ceccanti, A.; Laschi, F.; Zanello, P. *Inorg. Chim. Acta* **1997**, *259*, 61−70.
(57) Ramakrishnan, S.; Chakraborty, S.; Brennessel, W. W.; Chidsey, C. E. D.; Jones, W. D. *Chem. Sci.* **2016**, *7*, 117−127.
(58) Bourrez, M.; Steinmetz, R.; Ott, S.; Gloaguen, F.; Hammarstrom, L. *Nat. Chem.* **2015**, *7*, 140−145.
(59) Sunkel, K.; Urban, G.; Beck, W. *J. Organomet. Chem.* **1983**, *252*, 187−194.
(60) Cutler, A. R.; Todaro, A. B. *Organometallics* **1988**, *8*, 1782−1787.
(61) Uddin, M.; Lalia-Kantouri, M.; Hadjikostas, C. C.; Voutsas, G. *Z. Anorg. Allg. Chem.* **1998**, *624*, 750−753.
(62) Amani Komaei, S.; van Albada, G. A.; Haasnoot, J. G.; Kooijman, H.; Spek, A. L.; Reedijk, J. *Inorg. Chim. Acta* **1999**, *286*, 24−29.
(63) Esteban, D.; Banobre, D.; Bastida, R.; de Blas, A.; Macias, A.; Rodriguez, A.; Rodriguez-Blas, T.; Fenton, D. E.; Adams, H.; Mahia, J. *Inorg. Chem.* **1999**, *38*, 1937−1944.
(64) Hamstra, B. J.; Cheng, B.; Ellison, M. K.; Scheidt, W. R. *Inorg. Chem.* **1999**, *38*, 3554−3561.
(65) Cimadevilla, F.; Garcia, M. E.; Garcia-Vivo, D.; Ruiz, M. A.; Graiff, C.; Tiripicchio, A. *Inorg. Chem.* **2012**, *51*, 7284−7295.
(66) The reduction of complexes **1**−**4** is not observed by cyclic voltammetry within the solvent window, indicating that the Ru(I/II) couple is at potentials much more negative than −0.8 V versus $Fc^{0/+}$.
(67) While protonation of the Ru−hydride with isopropanol to generate the Ru−isopropoxide and dihydrogen has been established from chemical reactivity studies, this reaction is too slow at room temperature to be responsible for this second feature on the CV time scale.
(68) Nicholson, R. S.; Shain, I. *Anal. Chem.* **1964**, *36*, 706−723.
(69) Saveant, J. M.; Vianello, E. *Electrochim. Acta* **1965**, *10*, 905−920.
(70) Weiss, C. J.; Wiedner, E. S.; Roberts, J. A. S.; Appel, A. M. *Chem. Commun.* **2015**, *51*, 6172−6174.
(71) Helm, M. L.; Stewart, M. P.; Bullock, R. M.; DuBois, M. R.; DuBois, D. L. *Science* **2011**, *333*, 863−866.
(72) Sun, C.; Prosperini, S.; Quagliotto, P.; Viscardi, G.; Yoon, S. S.; Gobetto, R.; Nervi, C. *Dalton Trans.* **2016**, *45*, 14678−14688.
(73) Bonitatibus, P. J.; Rainka, M. P.; Peters, A. J.; Simone, D. L.; Doherty, M. D. *Chem. Commun.* **2013**, *49*, 10581−10583.
(74) Bonitatibus, P. J.; Chakraborty, S.; Doherty, M. D.; Siclovan, O.; Jones, W. D.; Soloveichik, G. L. *Proc. Natl. Acad. Sci. U. S. A.* **2015**, *112*, 1687−1692.
(75) Annen, S. P.; Bambagioni, V.; Bevilacqua, M.; Filippi, J.; Marchionni, A.; Oberhauser, W.; Schönberg, H.; Vizza, F.; Bianchini, C.; Grützmacher, H. *Angew. Chem., Int. Ed.* **2010**, *49*, 7229−7233.
(76) Bellini, M.; Bevilacqua, M.; Filippi, J.; Lavacchi, A.; Marchionni, A.; Miller, H. A.; Oberhauser, W.; Vizza, F.; Annen, S. P.; Grützmacher, H. *ChemSusChem* **2014**, *7*, 2432−2435.
(77) Badalyan, A.; Stahl, S. S. *Nature* **2016**, *535*, 406−406.
(78) Sheldrick, G. M. *Acta Crystallogr., Sect. A: Found. Crystallogr.* **2008**, *A64*, 112−122.
(79) *XL: Program for the Refinement of X-ray Crystal Structure, Part of the SHELXTL Crystal Structure Determination Package*; Bruker Analytical X-ray Systems Inc.: Madison, WI, 1995−99.

DOI: 10.1021/jacs.6b09705
J. Am. Chem. Soc. 2017, 139, 738−748